Performance Analysis and Evaluation of Frequency-Locked Loop for Weak GNSS Signals Based on Spectral Line Interpolation

LI CHENG[1], WENFEI GUO[2], CHI GUO[2], (Member, IEEE), AND JIANSHENG ZHENG[1,2]

[1]School of Electronic Information, Wuhan University, Wuhan 430079, China
[2]GNSS Research Center, Wuhan University, Wuhan 430079, China

Corresponding author: Chi Guo (guochi@whu.edu.cn)

ABSTRACT In order to track weak signals, GNSS receivers often use a frequency-locked loop (FLL) to track the carrier frequency. The performance of the frequency discriminator directly affects the receiver's signal tracking capability in the FLL. In weak signals, FFT is currently used to estimate the carrier frequency. However, the FFT has a fence effect. The signal length affects the accuracy of the frequency estimation. According to the problem of FFT frequency estimation with low accuracy, we introduce three frequency estimators, which have good frequency estimation performances under low signal-to-noise ratio for GNSS weak signal tracking and propose a carrier frequency tracking method. The article compares and analyzes the estimation error performance of different frequency discriminators in detail. The simulation experiments are used to verify and analyze the tracking sensitivity of the tracking loop under different carrier-to-noise ratios. Theoretical analysis and simulation results show that these estimators effectively improve the accuracy of frequency estimation compared to traditional FFT estimator. Using the open-loop tracking structure, the tracking sensitivity can reach 24 dB-Hz when the coherent integration time is 20 *ms* and the number of signal samples is 16. Adding a loop filter, the tracking threshold can be improved to 20 dB-Hz.

INDEX TERMS Frequency estimation, open loop tracking, RMSE, tracking threshold, weak signal tracking.

I. INTRODUCTION

The normal operation of the GNSS receiver is based on the stable tracking of the signal, including carrier tracking and pseudo-noise code (PN code) tracking. Due to the short wavelength of the carrier, carrier tracking has become the most vulnerable link in the receiver [1]. Currently, phase-locked loop (PLL) is often employed to track the carrier signal. The loop uses the local carrier to discriminate the phase of the received carrier. Then the phase delay of the local carrier can be detected. The local carrier aligns itself with the received signal by the feedback control of the local carrier generator. The phase-locked loop is the best tracking method when the signal environment is good. However, under weak signal environment, large phase noise often causes the tracking loop to lose lock. In order to improve the sensitivity of the tracking loop, the frequency-locked loop (FLL) is often

used to replace the phase-locked loop when the signal is weak [2]. Unlike the phase-locked loop, the frequency-locked loop only estimates the frequency error to achieve frequency locking. The frequency-locked loop that is not concerned about the phase error greatly improves the stability of the loop.

The performance of frequency tracking is to some extent depends on the frequency discriminator. Different frequency estimators directly affect the accuracy and sensitivity of frequency tracking. The frequency estimation is a fundamental problem in signal processing. Estimating the frequency of a complex sinusoidal signal has been extensively studied in the field of communications [3]–[8]. Using discrete Fourier transform (DFT) to estimate frequency is the classic estimation method in frequency domain. In order to alleviate the fence effect of DFT, some researchers proposed using a two-step search algorithm to fine the estimation [9]–[15]. Based on the index of peak value in the DFT magnitude spectrum, the adjacent frequency spectrum interpolation is used

The associate editor coordinating the review of this manuscript and approving it for publication was Zhen Ren.

L. Cheng *et al.*: Performance Analysis and Evaluation of FLL for Weak GNSS Signals Based on Spectral Line Interpolation

IEEE *Access*

to estimate the fractional correction term δ. Scholars strive to find a method with higher estimation accuracy, smaller frequency deviation and simple calculation. Quinn [11] proposed an interpolation method based on quadratic functions in 1994, which uses the amplitude and phase information of the two DFT coefficients on either side of the maximum bin. However, estimation error of the frequency deviation increases when the real frequency is close to the maximum frequency bin. To reduce the error of frequency deviation estimation, Macleod [12] proposed an improved algorithm. This algorithm removed the prediction of the frequency deviation polarity. Including the maximum value of the spectrum, the complex values of the two adjacent spectral lines are used to obtain a unique frequency estimation formula. A unique frequency estimation formula is implemented using the complex values of the two adjacent spectral lines and the maximum spectral line. Jacobsen and Kootsookos [13] proposed a calculation formula using three spectral lines for interpolation in 2007. The estimation formula is simple and easy in calculating. In 2011, Candan [14] derived Jacobsen's formula and gave the bias correction item, which improved the mean square error performance of the frequency estimator under high signal-to-noise ratio (SNR). Other estimation methods calculate the DFT utilizing zero-padding series in the time domain. The purpose is to ensure that the spectral lines used in calculating the frequency deviation are within the main lobe range. Rational Combination of Three Spectrum Lines (RCTSL) [15] uses the amplitudes of the maximum spectral line and its two neighbors to estimate the frequency after zero-padding. This method is based on least square approximation in frequency domain, which has a lower SNR threshold compared with other methods. As mentioned above, the methods with a small amount of calculation have better performance than DFT. They are suitable for GNSS signal frequency tracking. However, most of the existing researches aimed at improving the frequency bias performance under high SNR environment. Few of them are investigated the performance under low SNR environment, especially in the GNSS tracking loop.

This paper aims at the carrier tracking problem of weak GNSS signals. With a frequency tracking structure, we compared the tracking jitters and sensitivity under low SNR environment using different frequency estimation methods. Meanwhile, the relationship between the performance of open-loop/closed-loop tracking loop and the frequency estimators is analyzed. This paper is organized as follows: Section II introduces the GNSS carrier frequency tracking structure and three frequency estimation methods, which are suitable for the tracking loop. The performances of the three frequency estimators including frequency bias and root mean square error (RMSE) under different SNR environments are analyzed and compared in Section III. Section IV gives simulation results and compares the performance of different frequency estimators in the GNSS signal tracking loop. The sensitivity of the loop in open-loop and closed-loop structures

are given respectively. The last part summarizes the experiments and draws the conclusion of this article.

II. GNSS SIGNAL MODEL AND CARRIER TRACKING METHOD

In order to guarantee the signal power against loss, the integration limit of the signal cannot exceed the navigation data bit. The digitized IF signal received at the end of the GNSS receiver RF front-end for a visible GNSS satellite can be presented as [16]:

$$r(i) = A(iT_s) D(iT_s) \cdot C(iT_s - \tau)$$
$$\cdot \cos(2\pi T_s (f_{IF} + f_d) i + \phi) + n(iT_s) \quad (1)$$

where T_s is the sample period, τ denotes the code delay in samples, $\emptyset$ is the carrier phase, f_{IF} is the intermediate frequency, and f_d is the carrier Doppler frequency shift. $r(i)$ represents the received IF GNSS signal at the end of the RF front-end sampled at time $t = iT_s$, $D(iT_s)$ is the navigation data bits, $C(iT_s - \tau)$ stands for the spreading code sequence for GNSS. $n(iT_s)$ is the additional band-limited white Gaussian noise. The bilateral power spectral density of the white Gaussian noise is $N_0/2$. In practice, the GNSS receiver must use two loops to track the carrier and code phase simultaneously. The basic principles of the two loops are the same, except that the discriminators are different. Because the carrier frequency is much higher than the code frequency. Carrier tracking is often a weak link relative to code tracking in the receiver and needs to be considered. Among the carrier tracking methods, the classic method is using the FLL or PLL to estimate the frequency or phase of the signal in the field of communications. Fig. 1 represents PLL structure in Laplace domain. The structure includes a phase detector, a loop filter and a local oscillator. The main function of the phase-locked loop is to identify the phase difference between the local carrier signal and the received signal through the phase discriminator. PLL eliminates noise with filters and adjusts the frequency of the local oscillator to ensure the consistency of the local signal and the received signal.
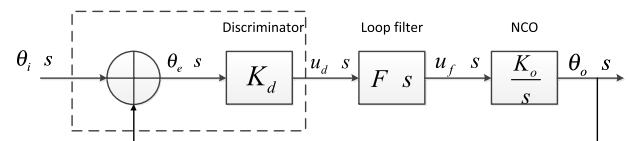

FIGURE 1. Typical tracking loop structure.

Generally, it is considered that the signal parameters $(A(t), \tau, \emptyset, f_d)$ change slowly. Therefore, the tracking performance is stable. For high dynamic and weak GPS signal environments, improved or more robust tracking methods are often applied, such as FLL-assisted-PLL, Kalman filter-based tracking method, etc. The methods that are widely used in the existing GNSS receivers have improved the
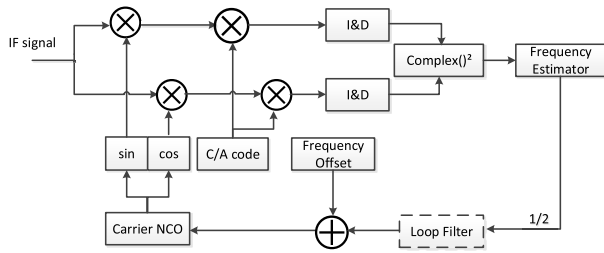
IEEE *Access*

L. Cheng *et al.*: Performance Analysis and Evaluation of FLL for Weak GNSS Signals Based on Spectral Line Interpolation

FIGURE 2. Carrier frequency tracking structure based on spectral analysis.

tracking performance of the receiver to some extent. In the tracking loop structure, the role of the loop filter is to eliminate noise. Thus, the accuracy of the local oscillator can be improved. In 2003, Krasner [17] proposed an open-loop tracking method, which can deal with urban canyons and weak indoor signals. This method improved the effectiveness of the receiver. We slightly modify the structure of the tracking method as shown in Fig. 2. The incoming IF signal mixed with local replicas of carrier and down-converted to the baseband. When the correlation operation with local replicas of code are accomplished, the residual complex carrier signals are integrated in the integrate-and-dump circuits. Then, the data bits can be removed after the complex square operation. We replace the spectral analysis block with the frequency estimator, which can estimate the Doppler. Then, the Doppler residual is used to tune the main carrier numerically-controlled oscillator (NCO) after addition to the frequency offset. Unlike traditional tracking methods, open-loop tracking only estimates the Doppler frequency, and directly uses the estimated frequency to control the local NCO, without the loop filter in the conventional loop. Since there is no smoothing of the filter, the amount of frequency adjustment each time is determined by the estimated frequency. The Doppler frequency is determined by performing FFT after the complex square operation.

A. CARRIER TRACKING STRUCTURE
Since the GNSS navigation is 50 bps the coherent integration time of the signal is up to 20 *ms* without the assistance of external information. The tracking loop structure in Fig. 1 can be expanded into Fig. 2:

When the code loop is working well, the spreading code $C(iT_s - \tau)$ can be removed by the prompt code. The IF signal in (1) could be simplified as the following complex signal:

$$r(t) = AD(t)\cos(2\pi f_e t + \phi_e) + j\sin(2\pi f_e t + \phi_e) + n(t) \quad (2)$$

Ignoring high frequency information items and within one bit interval, the output of the integrate-and-dump circuit can be expressed as:

$$s(t) = AD(t)\,sinc(\pi f_e T_{coh})\,e^{j\left[2\pi f_e\left(t+\frac{T_{coh}}{2}\right)+\phi_e\right]} + n(t) \quad (3)$$

where T_{coh} stands for the coherent integration time, $sinc(x)$ function is defined as $sinc(x) = sin(x)/x$. In the local NCO update period, the above formula can be regarded as a simple

BPSK signal. The effect of data bit can be eliminated by squaring the operation [18], after which a complex cosine signal can be obtained with noises being ignored:

$$y(t) = A^2 sinc^2\left(\pi f_e T_{coh}\right) e^{j\left[2\pi * 2f_e\left(t+\frac{T_{coh}}{2}\right)+2\phi_e\right]} \quad (4)$$

Note that $y(t)$ contains only one spectral line at frequency $2f_e$. The frequency could be detected by FFT as an effective method in the frequency domain. The detected frequency is used to adjust the NCO and then track the carrier frequency. In order to improve the estimation performance, we intend to use FFT to get a coarse estimation. The fine estimation is implemented by the spectral line interpolation methods mentioned above. Finally an accurate frequency discriminator is formed.

B. FREQUENCY ESTIMATION METHOD
In (4), ignoring the short-term amplitude change, the input of the frequency discriminator can be regarded as a complex sinusoidal signal with single-tone. Therefore, (4) is simplified as:

$$y(t) = A_0 e^{j(2\pi f_0 t + \theta_0)}, \quad 0 \le t \le T \quad (5)$$

where A_0, f_0, and θ_0 are the amplitude, frequency, and phase of the signal. T is signal observation time. In order to describe the frequency estimation method of a complex sinusoidal signal, we give Fig. 3 to show the DTFT and DFT of a single-tone signal in the absence of noise.
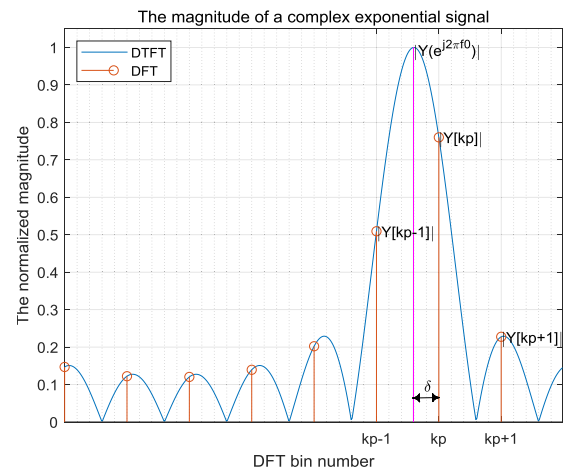

FIGURE 3. DTFT and DFT spectrum of a signal complex tone without noise.

It can be seen from Fig. 3, due to the truncation effect of time domain signal, the spectrum of the sinusoidal signal is not a single tone any more. It expands into a narrow band signal with a main lobe width of $2/T$. This brings difficulties to frequency estimation using DFT. In Fig. 3, $\left|Y\left(e^{j2\pi f_0}\right)\right|$ is the peak of DTFT, $Y[k_p]$ is the maximum magnitude of DFT. δ is the index deviation between the maximum magnitude and the real frequency, with the constraint that $-0.5 < \delta < 0.5$.

L. Cheng *et al.*: Performance Analysis and Evaluation of FLL for Weak GNSS Signals Based on Spectral Line Interpolation

IEEE *Access*

So, the estimated frequency can be written as:

$$\hat{f}_0 = \left(k_p + \hat{\delta}\right)\frac{f_s}{N} \tag{6}$$

where k_p is the index of the maximum amplitude, f_s/N is discrete frequency interval. In the noiseless case, the DFT of the complex sinusoidal signal $y(t)$ can be expressed as follows:

$$Y[k] = \sum_{n=0}^{N-1} A_0 e^{j(2\pi f_0 n/f_s + \theta_0)} e^{-j(2\pi/N)nk}$$
$$(k = 0, 1, \ldots, N-1) \tag{7}$$

Carrying out the necessary manipulations [19], we obtain:

$$Y[k_p + m] = A_0 e^{j\theta_0} e^{j\pi \frac{N-1}{N}(\delta - m)} \frac{\sin[\pi(\delta - m)]}{\sin[\pi(\delta - m)/N]} \tag{8}$$

where m is a real number. When $m = 0$, we can get $Y[k_p]$:

$$Y[k_p] = A_0 e^{j\theta_0} e^{j\pi \frac{N-1}{N}\delta} \frac{\sin[\pi\delta]}{\sin[\pi\delta/N]} \tag{9}$$

for $m = \pm 1$, the two neighbors of the maximum DFT spectral line $Y[k_p]$ are as follows:

$$Y[k_p + 1] = A_0 e^{j\theta_0} e^{j\pi \frac{N-1}{N}(\delta - 1)} \frac{\sin[\pi(1-\delta)]}{\sin[\pi(1-\delta)/N]} \tag{10}$$

$$Y[k_p - 1] = A_0 e^{j\theta_0} e^{j\pi \frac{N-1}{N}(\delta + 1)} \frac{\sin[\pi(1+\delta)]}{\sin[\pi(1+\delta)/N]} \tag{11}$$

Besides the index of the maximum magnitude, the frequency estimation of the complex sinusoidal signal needs the assistance of $Y[k_p + 1]$ and $Y[k_p - 1]$ on the left and right sides of the maximum spectral line. Then the frequency deviation δ of the fractional part can be accurately estimated. The first coarse estimation of the two-step method is to obtain the magnitude spectrum through DFT, and select the index value k_p as the coarse estimation. In the second step, the fine estimation uses the estimation algorithm of δ to estimate the fine part of the frequency.

Many scholars proposed using quadratic function to interpolate the spectral lines next to the highest amplitude value to achieve a fine estimation. In 1998, Macleod [12] proposed a frequency estimator using the peak value of DFT and its adjacent spectral lines. The algorithm removes the prediction of the positive and negative polarity of δ by cross-multiplying between the spectral lines.

$$\gamma = \frac{Re\left\{Y[k_p - 1]Y^*[k_p] - Y[k_p + 1]Y^*[k_p]\right\}}{Re\left\{2|Y[k_p]|^2 + Y[k_p - 1]Y^*[k_p] + Y[k_p + 1]Y^*[k_p]\right\}} \tag{12}$$

$$\hat{\delta} \approx \frac{\left(\sqrt{1 + 8\gamma^2} - 1\right)}{4\gamma} \tag{13}$$

This algorithm will not bring greater deviation due to the polarity estimation inaccuracy around $\delta = 0$.

In 2007, Jacobsen and Kootsookos [13] used the complex values of the three spectral lines instead of the amplitude to correct the frequency estimate, resulting in an estimate

formula for the frequency deviation. In 2011, Candan [14] carried out detailed derivation and coefficient correction of Jacobsen's formula. The correction item makes the frequency estimation deviation of Candan's method much more accuracy than that of Jacobsen's method. The frequency estimate δ can be expressed as:

$$\hat{\delta} = \frac{\tan \pi/N}{\pi/N} Re\left\{\frac{Y[k_p - 1] - Y[k_p + 1]}{2Y[k_p] - Y[k_p - 1] - Y[k_p + 1]}\right\} \tag{14}$$

Since Candan's algorithm reduces the bias of frequency estimation, the RMSE performance of the frequency estimator has been significantly improved at high SNR.

It can be seen that the previous methods use the real part of spectral line interpolation to estimate δ. These methods are mainly used to reduce bias, and focus on a high signal-to-noise ratio environment. Aiming at the frequency estimation at low signal-to-noise ratio environment, in 2011, Yang and Wei [15] used the least squares approximation method to estimate the sinusoidal signal power spectrum in the frequency domain. The RCTSL algorithm was proposed.

$$\hat{\delta} = \frac{N}{\pi} \frac{|Y[k_p + 1]|^2 - |Y[k_p - 1]|^2}{u\left(|Y[k_p + 1]|^2 + |Y[k_p - 1]|^2\right) + v|Y[k_p]|^2} \tag{15}$$

where u and v are constant coefficients, which only related to the signal length. Their optimal weight coefficients are also given:

$$u = \frac{64N}{\pi^5 + 32\pi} \tag{16}$$

$$v = \frac{u\pi^2}{4} \tag{17}$$

By means of zero padding, RCTSL can effectively improve the frequency estimation accuracy under low signal-to-noise ratio compared to the other methods.

Compared with the traditional FFT frequency estimation, the above methods use spectral line interpolation to estimate δ after locating the index with the maximum magnitude in frequency domain. Thereby these methods improve the accuracy of frequency estimation. However, these studies only analyzed the frequency estimation performance at high SNR. The performance at low SNR, especially when applied to GNSS tracking loops, has not been thoroughly analyzed. This article applies these methods to the frequency-locked loop in GNSS weak signal tracking, expecting for a higher tracking sensitivity.

III. PERFORMANCE ANALYSIS

Since the exact relationship between the frequency offset and the DFT coefficient interpolation is nonlinear, most of these direct interpolation approaches cause estimation bias inevitably [20] Moreover, in practice, signals are always mixed with noise, causing the results to fluctuate in a certain range. In this case, the RMSE has two components [21]:

$$RMSE = \sqrt{\sigma^2 + bias^2} \tag{18}$$

σ^2 results from additive white noise and the bias is caused by the linearization of the interpolation. The performance of frequency estimator is mainly determined by noise at low SNR, whereas the performance is mainly restricted by the bias at high SNR. When the signal's phase is unknown, the Cramer Rao lower bound (CRLB) [22] of the frequency estimates can be derived from the maximum likelihood (ML) estimation method:

$$\sigma_f^2 = \frac{6f_s^2}{(2\pi)^2 N \left(N^2 - 1\right) SNR} \tag{19}$$

where N is the number of signal samples f_s is the sampling frequency and SNR is the signal-to-noise ratio. The accuracy of frequency estimation will be enhanced by larger observation window size or higher SNR. Although CRLB is derived from the ML estimator that is unbiased, σ_f is still a reference for the RMSE performance of the frequency estimator whether or not it is biased.

Since our goal is improving the tracking sensitivity of the GNSS receiver, the following experiments focus on the performance of three frequency estimators from −10 dB to 30 dB. In this section, we compare the bias of three different frequency estimators without noise, RMSE performance with respect to different delta and RMSE performance with respect to SNR. The same simulation parameters in the following simulation experiments are: $f_s = 1KHz, f_0 = \left(N/4 + \delta\right) * f_s/M$, N is the number of samples and M is M-point DFT. For example, $N = 8$, then the true frequency in Candan and Macleod methods is $187.5Hz < f_0 < 312.5Hz$

A. BIAS OF DIFFERENT ESTIMATORS IN THE ABSENCE OF NOISE

First, we compare the bias of three frequency estimators. We set the noise to zero and $0 < \delta < 0.5$. In Candan and Macleod's methods, N and M equal 8. However, RCTSL needs16-point FFT after zero-padding. The simulation results are shown in Fig. 4:
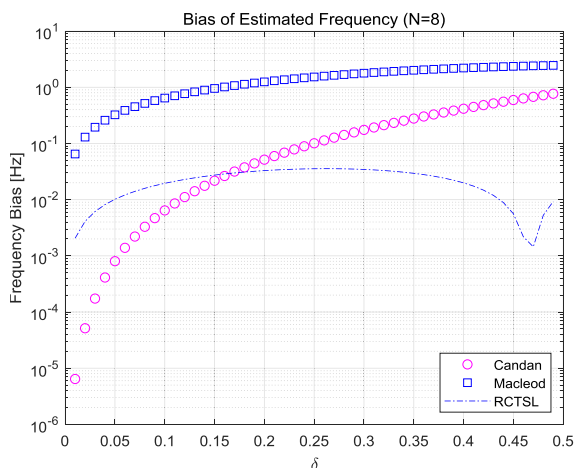

FIGURE 4. Noiseless bias performance comparison (*N* = 8).

Frequency estimation is a nonlinear estimation problem. Therefore, it can be seen from Fig. 4 that the mentioned frequency estimators are all biased. The frequency bias values of Macleod and Candan estimators are monotonically increasing as δ increases. As the true frequency near the center of two adjacent frequency bins, the bias becomes larger. The minimum bias value of RCTSL is obtained at $\delta = 0.47$. The frequency bias of RCTSL tends to be stable between the adjacent spectral lines. When $0 < \delta \leq 0.16$, Candan estimator is the least biased estimator. When $0.16 < \delta < 0.5$ RCTSL estimator is the least biased estimator. The poorest bias belongs to the Macleod estimator. It's worth pointing out that RCTSL estimator represents half physical frequency versus two other estimators with the same value of δ. This is due to zero-padding in RCTSL.

The bias of Macleod estimator, Candan estimator and RCTSL estimator versus δ are shown in Fig. 5 for $N = 16$. Other parameters remain unchanged. Comparing Fig. 4 and Fig. 5, the frequency bias of the three estimators gets smaller as N increases. Macleod estimator has the poorest bias of the three. The frequency bias of RCTSL is still non-monotonic. The minimum bias value of RCTSL appears at $\delta = 0.21$.
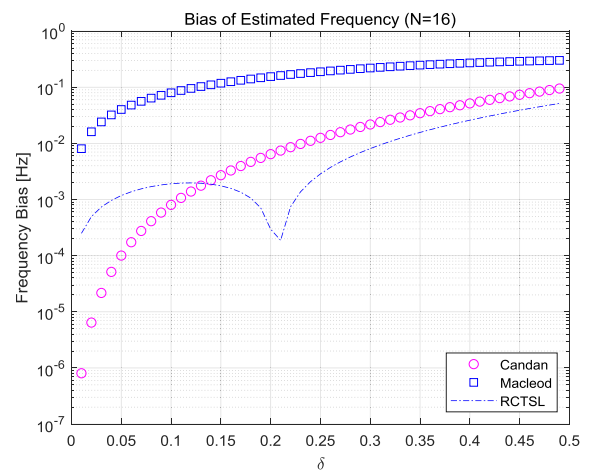

FIGURE 5. Noiseless bias performance comparison (*N* = 16).

B. RMSE PERFORMANCE OF DIFFERENT ESTIMATORS WITH RESPECT TO DIFFERERNT DELTA

In this experiment Gaussian white noise is added to the signal while δ varies from −0.5 to 0.5. We compare the frequency RMSE of these three estimators for $N = 8$ and $SNR = 5dB$. Each experiment is repeated 1000,000 times and RMSE is calculated.

From Fig. 6, we can see that the RMSE curve of Candan and Macleod estimators follows the same trend with respect to different δ. At small δ, RMSE performance of Candan and Macleod are better than each performance at large δ. The two estimators have the poorest frequency RMSE as δ is close to 0.5. Different from noiseless condition, the RMSE of Candan estimator is worse than Macleod estimator for $SNR = 5dB$.
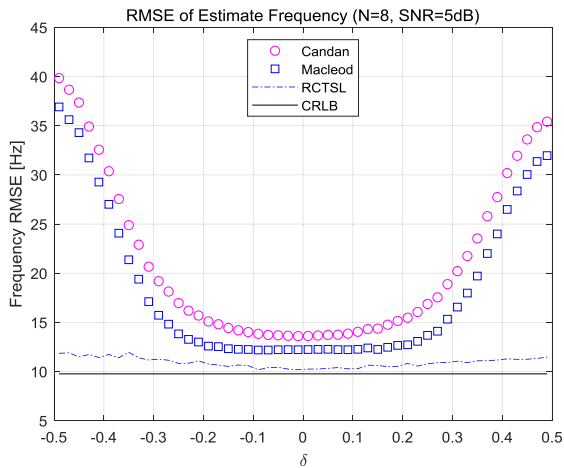
L. Cheng *et al.*: Performance Analysis and Evaluation of FLL for Weak GNSS Signals Based on Spectral Line Interpolation

IEEE *Access*

FIGURE 6. RMSE performance comparison with respect to different δ ($N = 8$, SNR = 5dB).
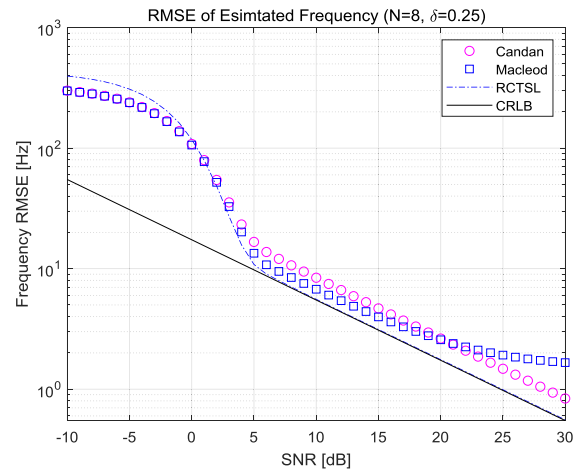

FIGURE 8. RMSE performance comparison with respect to SNR ($N = 8$, $\delta = 0.25$).
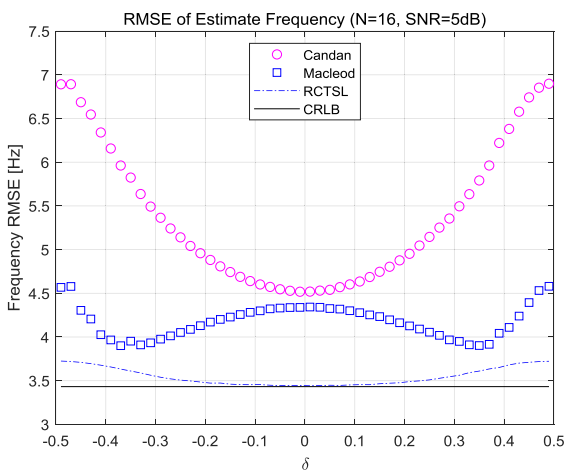

FIGURE 7. RMSE performance comparison with respect to different δ ($N = 16$, SNR = 5dB).

This is associated with deficient noise resistant of Candan estimator in noisy cases. The RMSE of RCTSL estimator is almost independent of δ and is closer to the CRLB than the other estimators are.

The frequency RMSE of Macleod estimator, Candan estimator and RCTSL estimator versus δ are shown in Fig. 7 for $N = 16$. Other parameters remain unchanged. It can be seen that RMSE decreases significantly as the observation N increases. The RMSE performance of Candan estimator is the worst of the three. The RMSE performance of RCTSL estimator is the best. Macleod estimator and Candan estimator have similar performance around $\delta = 0$. However, the performance gap between the two gradually widens as δ increases. The frequency RMSE of Candan estimator is close to 7 Hz as δ approaches 0.5. The RMSE of RCTSL estimator is very close to the CRLB around $\delta = 0$. The frequency RMSE of RCTSL estimator is about 3.7Hz when δ is close to 0.5. The behavior of RCTSL estimator follows the stable trend at different δ.

C. RMSE PERFORMANCE OF DIFFERENT ESTIMATORS WITH RESPECT TO SNR

This experiment compares the frequency RMSE of different estimators with respect to SNR in the range of -10dB to 30dB. The parameter δ is fixed to a specific value, which is $\delta = 0.25$. The number of Monte Carlo simulations is 1000,000 times. Meanwhile, we draw the CRLB as an analysis reference of the frequency RMSE performance. We plot the frequency RMSE curve of these three estimators for $N = 8$ and $N = 16$ respectively.

Fig. 8 shows the frequency RMSE of the three estimators and the CRLB with respect to different SNR for $N = 8$. The RMSE floor of Macleod estimator occurs at $SNR = 30dB$. Because at high SNR, the estimator bias is the dominated factor of the RMSE. It can be noted from this figure that the RMSE curve of RCTSL estimator is close to the CRLB when the SNR varies from 5dB to 30dB. The performance of the three estimators display a sudden drop at $SNR = 5dB$. The high RMSE of the simulated results at low SNR is due to an incorrect peak selected in the spectrum. From Fig. 8, we can see that the SNR threshold of the three estimators is 5dB for $N = 8$. Meanwhile, the frequency RMSE is about 10Hz.

In Fig. 9, we present a frequency RMSE comparison of the three estimators for a larger number of observation samples which is $N = 16$. The RMSE performance of the three frequency estimators obviously improves as N increases. The RMSE curves of all the estimators are close to the CRLB when the SNR varies from 3 dB to 25dB. The RMSE of RCTSL estimator is the best. The RMSE of the three estimators drops rapidly and departs from the CRLB curve, when the SNR is lower than 3 dB. It can be noted from this figure that the SNR threshold of the three estimators is 2dB for $N = 16$. Meanwhile, the frequency RMSE is about 5 Hz.

In the simulation experiments above, the RMSE performance of RCTSL estimator is closer to the CRLB than the competing estimators. At low SNR, RCTSL estimator has the smallest frequency estimation deviation. Next, we simulate
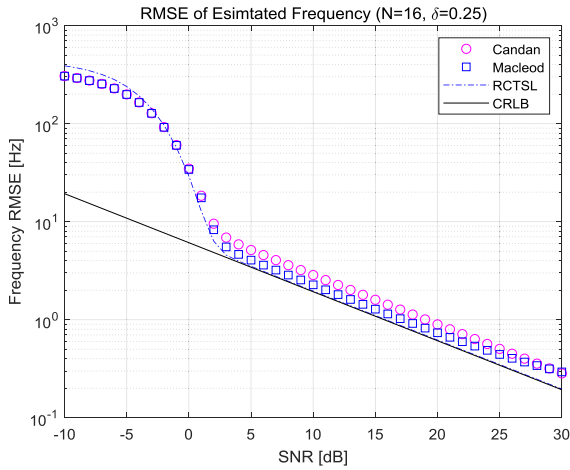
IEEE *Access*

L. Cheng *et al.*: Performance Analysis and Evaluation of FLL for Weak GNSS Signals Based on Spectral Line Interpolation

FIGURE 9. RMSE performance comparison with respect to SNR ($N = 16$, $\delta = 0.25$).

FIGURE 10. Tracking jitter of different frequency discriminators with $N = 8$.

FIGURE 11. Tracking jitter of different frequency discriminators with $N = 16$.

the tracking performance of GNSS weak signal using proposed carrier tracking structure and different frequency estimators. Then we can explore the effect of different frequency estimators on GNSS signal tracking performance.

IV. NUMERICAL RESULTS

The carrier-tracking loop adopts the frequency-locked loop structure shown in Fig. 2. The coherent integration time in the loop is 20ms. The carrier-to-noise ratio varies from 16 dB-Hz to 40 dB-Hz. In order to eliminate the effect of data bit inversion, the complex square is carried out after coherent integration. Moreover, 8 points or 16 points sampled values are adopted as the inputs of the frequency discriminator after being complex squared. The frequency discriminator employs Candan, Macleod, RCTSL estimators. For comparison, the common FFT estimator and Differential Power (DP) frequency discriminator [23] are also tested. In addition, we test the tracking performance of GNSS signals through the semi-simulation platform [24].

A. OPEN LOOP TRACKING PERFORMANCE

First, the loop filter in Fig. 2 is removed. We simulate the open-loop tracking performance. The tracking performance mainly depends on the frequency estimator without the smoothing effect of the loop filter. Fig. 10 and Fig. 11 are the comparison graphs of tracking jitter performance for $N = 8$ and $N = 16$.

As shown in Fig. 10, for $N = 8$, the tracking threshold of the FFT estimator is about 30 dB-Hz. The tracking jitter of the FFT estimator is the biggest. Candan, Macleod and differential power frequency discriminators have a 28 dB-Hz tracking thresholds. The tracking jitter of Candan estimator has similar performance with Macleod estimator. DP discriminator has the smallest tracking jitter. RCTSL estimator can track the carrier-to-noise ratio of 26 dB-Hz. It has similar performance of tracking jitter with DP discriminator. RCTSL estimator outperforms the other estimators for $N = 8$. In the simulation, the coherent time is 20 *ms* and the noise bandwidth is 100 *Hz*.
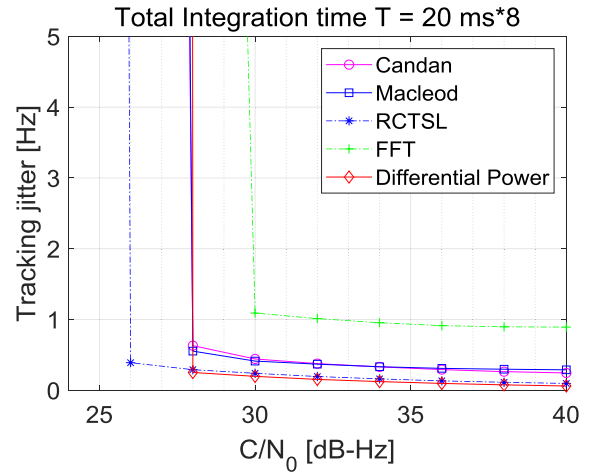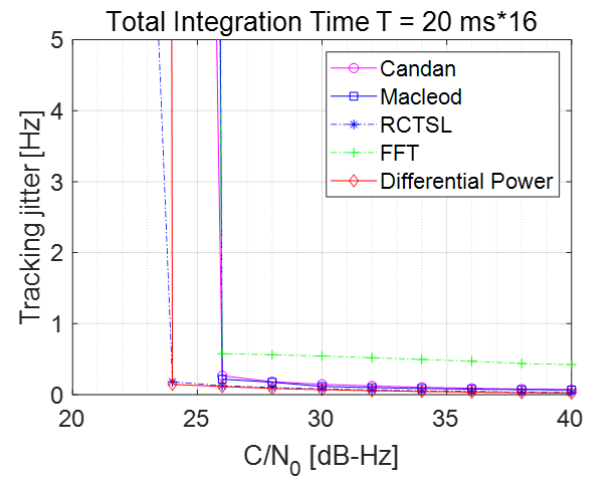
Thus, 26 dB-Hz in carrier-to-noise ratio is corresponding to about 6 dB in SNR. This is consistent with the SNR threshold in Fig. 8.

Fig. 11 is a comparison of tracking jitter for different frequency discriminators for $N = 16$. Fig. 11 shows that the tracking threshold and tracking jitter of all frequency discriminators decrease as N increases. FFT, Candan and Macleod discriminator have a 26 dB-Hz tracking threshold. The jitter of FFT discriminator is the biggest. The jitter of Candan discriminator is close to the jitter of Macleod discriminator. The tracking threshold of RCTSL and DP discrimination is about 24 dB-Hz. They have similar tracking jitter. As the noise bandwidth is 100 Hz, 24 dB-Hz in carrier-to-noise ratio is corresponding to about 4 dB in SNR. This simulation is consistent with the SNR threshold in Fig. 9.

B. CLOSED LOOP TRACKING PERFORMANCE

For weak signals, the loop filter can reduce the influence of noise and improve the output accuracy of the frequency discriminator. To verify the sensitivity performance of the

L. Cheng *et al.*: Performance Analysis and Evaluation of FLL for Weak GNSS Signals Based on Spectral Line Interpolation

IEEE *Access*

FIGURE 12. Tracking jitter of different frequency discriminators with
N = 8.

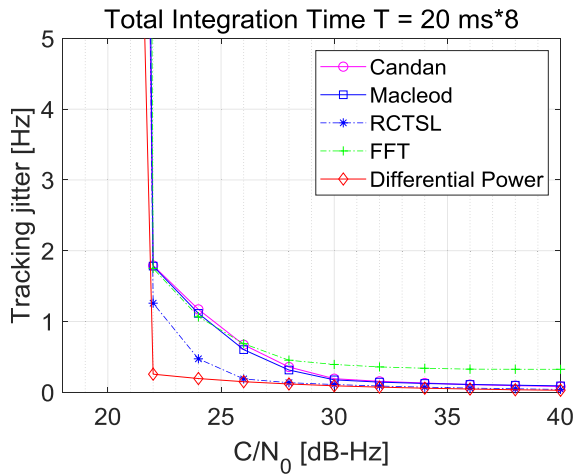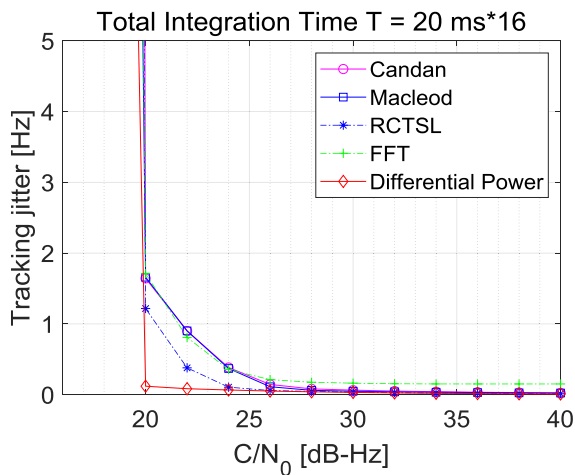**FIGURE 13.** Tracking jitter of different frequency discriminators with
N = 16.

carrier tracking loop, a loop filter is added to the tracking structure of Fig. 2. We compare the tracking jitter performances of different frequency estimators in the closed loop. In this simulation, we set the loop filter as the first-order filter. We use 8 outputs of the square operation. The bandwidth of the loop filter is 2Hz. Fig. 12 shows the tracking jitters of different frequency discriminators. From Fig. 12, we can see that the tracking thresholds of all frequency discriminators are improved to 22 dB-Hz under the effect of the loop filter. Nevertheless, different frequency discriminators have different frequency deviations. Under 26 dB-Hz, FFT discriminator is the worst. DP discriminator is the best. Above 26 dB-Hz, the tracking jitter performances of DP discriminator and RCTSL discriminator are almost the same.

The simulation parameters of Fig. 13 and Fig. 12 are the same, except for using 16 outputs of the square operation. Meanwhile, the bandwidth of the loop filter is set to 1Hz. It can be noted from this figure that the tracking jitter performances of all discriminators are improved compared to Fig. 12. The tracking threshold is improved to 20 dB-Hz.

V. CONCLUSION

In order to improve the carrier tracking sensitivity of the GNSS receiver in a weak signal environment, we introduced three frequency estimators as the frequency discriminators into the field of GNSS weak signal tracking. Moreover, we propose a carrier frequency tracking structure. In this paper, we compare the bias and RMSE performance of different estimators. Then, we analyze the tracking sensitivity of the tracking loop under different parameters through semi-analytical techniques. Experiments show that RCTSL estimator can track a lower threshold signal of 24 dB-Hz in carrier-to-noise ratio than other estimators for *N* = 16. After adding the loop filter, the improved tracking threshold rise to 20 dB-H*z*. Among all the frequency estimators mentioned above, RCTSL and DP frequency discrimination have similar tracking performances and have the highest tracking sensitivities. The research findings have important implications for the Doppler estimation of the GNSS signal and the accuracy of the speed estimation of the receiver.

REFERENCES

[1] P. W. Ward, J. W. Betz, and C. J. Hegarty, "Satellite signal acquisition, tracking, data demodulation," in *Understanding GPS Principles and Applications*, vol. 5. Norwood, MA, USA: Artech House, 2006, pp. 153–241.

[2] P. W. Ward, "Performance comparisons between FLL, PLL and a novel FLL-assisted-PLL carrier tracking loop under RF interference conditions," in *Proc. ION GPS*, Nashville, TN, USA, 1998, pp. 783–795.

[3] E. Aboutanios and B. Mulgrew, "Iterative frequency estimation by interpolation on Fourier coefficients," *IEEE Trans. Signal Process.*, vol. 53, no. 4, pp. 1237–1242, Apr. 2005.

[4] Ç. Candan, "Fine resolution frequency estimation from three DFT samples: Case of windowed data," *Signal Process.*, vol. 114, pp. 245–250, Sep. 2015.

[5] D. Belega and D. Petri, "Frequency estimation by two- or three-point interpolated Fourier algorithms based on cosine windows," *Signal Process.*, vol. 117, pp. 115–125, Dec. 2015.

[6] J.-R. Liao and C.-M. Chen, "Phase correction of discrete Fourier transform coefficients to reduce frequency estimation bias of single tone complex sinusoid," *Signal Process.*, vol. 94, pp. 108–117, Jan. 2014.

[7] S. Gholami, A. Mahmoudi, and E. Farshidi, "Two-stage estimator for frequency rate and initial frequency in LFM signal using linear prediction approach," *Circuits, Syst., Signal Process.*, vol. 38, no. 1, pp. 105–117, Jan. 2019.

[8] C. L. Rino, K. M. Groves, C. S. Carrano, J. H. Gunter, and R. T. Parris, "Digital signal processing for ionospheric propagation diagnostics," *Radio Sci.*, vol. 50, no. 8, pp. 837–851, Aug. 2015.

[9] L. Fan and G. Qi, "Frequency estimator of sinusoid based on interpolation of three DFT spectral lines," *Signal Process.*, vol. 144, pp. 52–60, Mar. 2018.

[10] L. Fang, D. Duan, and L. Yang, "A new DFT-based frequency estimator for single-tone complex sinusoidal signals," in *Proc. IEEE Mil. Commun. Conf. (MILCOM)*, Orlando, FL, USA, Oct. 2012, pp. 1–6.

[11] B. G. Quinn, "Estimating frequency by interpolation using Fourier coefficients," *IEEE Trans. Signal Process.*, vol. 42, no. 5, pp. 1264–1268, May 1994.

[12] M. D. Macleod, "Fast nearly ML estimation of the parameters of real or complex single tones or resolved multiple tones," *IEEE Trans. Signal Process.*, vol. 46, no. 1, pp. 141–148, Jan. 1998.

[13] E. Jacobsen and P. Kootsookos, "Fast, accurate frequency estimators [DSP tips & tricks]," *IEEE Signal Process. Mag.*, vol. 24, no. 3, pp. 123–125, May 2007.

[14] Ç. Candan, "A method for fine resolution frequency estimation from three DFT samples," *IEEE Signal Process. Lett.*, vol. 18, no. 6, pp. 351–354, Jun. 2011.

IEEE *Access*

L. Cheng *et al.*: Performance Analysis and Evaluation of FLL for Weak GNSS Signals Based on Spectral Line Interpolation

[15] C. Yang and G. Wei, "A noniterative frequency estimator with rational combination of three spectrum lines," *IEEE Trans. Signal Process.*, vol. 59, no. 10, pp. 5065–5070, Oct. 2011.

[16] W. Guo, K. Yan, H. Zhang, X. Niu, and C. Shi, "Double stage NCO-based carrier tracking loop in GNSS receivers for city environmental applications," *IEEE Commun. Lett.*, vol. 18, no. 10, pp. 1747–1750, Oct. 2014.

[17] N. F. Krasner, "Method for open loop tracking GPS signals," U.S. Patent 6 633 255, Oct. 14, 2003.

[18] D. Borio and G. Lachapelle, "A non-coherent architecture for GNSS digital tracking loops," *Ann. Telecommun.-Annales des télé Commun.*, vol. 64, nos. 9–10, pp. 601–614, May 2009.

[19] U. Orguner and Ç. Candan, "A fine-resolution frequency estimator using an arbitrary number of DFT coefficients," *Signal Process.*, vol. 105, pp. 17–21, Dec. 2014.

[20] J.-R. Liao and S. Lo, "Analytical solutions for frequency estimators by interpolation of DFT coefficients," *Signal Process.*, vol. 100, pp. 93–100, Jul. 2014.

[21] C. Candan, "Analysis and further improvement of fine resolution frequency estimation method from three DFT samples," *IEEE Signal Process. Lett.*, vol. 20, no. 9, pp. 913–916, Sep. 2013.

[22] D. Rife and R. Boorstyn, "Single tone parameter estimation from discrete-time observations," *IEEE Trans. Inf. Theory*, vol. 20, no. 5, pp. 591–598, Sep. 1974.

[23] J.-C. Juang and Y.-H. Chen, "Phase/frequency tracking in a GNSS software receiver," *IEEE J. Sel. Topics Signal Process.*, vol. 3, no. 4, pp. 651–660, Aug. 2009.

[24] D. Borio, P. B. Anantharamu, and G. Lachapelle, "SATLSim: A semi-analytic framework for fast GNSS tracking loop simulations," *GPS Solutions*, vol. 15, no. 4, pp. 427–431, May 2011.

WENFEI GUO received the Ph.D. degree in communication and information system from Wuhan University, in 2011. He is currently an Associate Professor with the GNSS Research Center, Wuhan University. His research interests include GNSS receiver and relevant signal processing technologies, including high precise timing receivers, GNSS-R receivers, and anti-jamming receivers.

CHI GUO (Member, IEEE) received the M.Eng. and Ph.D. degrees in computer science from Wuhan University, Hubei, China. He is currently an Associate Professor with the National Satellite Positioning System Engineering Technology Research Center, Wuhan University. His current research interests include Beidou application, unmanned system navigation, and location-based services (LBSs).

JIANSHENG ZHENG received the B.S. and M.S. degrees in electrical technology, signal processing, and geodesy from Wuhan University, in 1982, 1999, and 2006, respectively. Since 1997, he has been a Professor with the School of Electronic Information, Wuhan University. His research interests include satellite navigation and positioning technologies, wireless communication technologies, and space optical communication technologies.

LI CHENG received the Ph.D. degree in communication and information system from Harbin Engineering University, in 2014. She is currently a Postdoctoral Fellow with the School of Electronic Information, Wuhan University. Her research interests include wireless communication, GNSS receiver, and relevant signal processing technologies.

• • •